文章编号：1001-9014(2024)01-0044-08

DOI:10.11972/j.issn.1001-9014.2024.01.007

Effects of Gamma irradiation on performance of InGaAsP/InP single-photon avalanche diodes

SUN Jing-Hua[1], WANG Wen-Juan[2*], ZHU Yi-Cheng[2,3], GUO Zi-Lu[2,3], QI Yu-Fei[2,3,5], XU Wei-Ming[4]

(1. School of Materials and Chemistry, the University of Shanghai for Science and Technology, Shanghai 200093, China;
2. State Key Laboratory of Infrared Physics, Shanghai Institute of Technical Physics, Chinese Academy of Sciences, Shanghai 200083, China;
3. University of Chinese Academy of Sciences, Beijing 100049, China;
4. Key Laboratory of Space Active Opto-Electronics Technology, Shanghai Institute of Technical Physics, Chinese Academy of Sciences, Shanghai 200083, China;
5. Hangzhou Institute for Advanced Study, University of Chinese Academy of Sciences, Hangzhou 310024, China)

Abstract: InGaAsP/InP single-photon avalanche diodes (SPADs) were gamma-irradiated with total doses of 10 krad (Si) and 20 krad (Si) and tested in situ and shift methods. After irradiation, the dark currents and dark count rates were degraded slightly, whereas the photon detection efficiency and the after pulse probability were basically unchanged. After a certain period of annealing at room temperature, these degradations were essentially recovered, indicating that transient ionization damage dominated in the gamma irradiation of InGaAsP/InP single-photon avalanche diodes.

Key words: Gamma irradiation, InGaAsP/InP, single-photon avalanche diode, single-photon performance

γ辐照对InGaAsP/InP单光子雪崩探测器性能的影响

孙京华[1], 王文娟[2*], 诸毅诚[2,3], 郭子路[2,3], 祁雨菲[2,3,5], 徐卫明[4]

(1. 上海理工大学 材料与化学学院,上海 200093;
2. 中国科学院上海技术物理研究所 红外物理国家重点实验室,上海 200083;
3. 中国科学院大学,北京 100049;
4. 中国科学院上海技术物理研究所 空间主动光电技术重点实验室,上海 200083;
5. 中国科学院大学杭州高等研究院,浙江 杭州 310024)

摘要:对InGaAsP/InP单光子雪崩探测器(SPADs)进行了总剂量为10 krad(Si)和20 krad(Si)的γ辐照,并进行了原位和移位测试。辐照后,暗电流和暗计数率有轻微的下降,而探测效率和后脉冲概率基本不变。经过一定时间的室温退火后,这些退化基本恢复,这表明瞬态电离损伤在γ辐照对InGaAsP/InP单光子雪崩探测器的损伤中占主导地位。

关 键 词:γ辐照;InGaAsP/InP;单光子雪崩探测器;单光子性能

中图分类号:TN312+.7　　**文献标识码**:A

Received date: 2023-03-31, **revised date**: 2023-11-06　　**收稿日期**:2023-03-31,**修回日期**:2023-11-06

Foundation items: Supported by the National Natural Science Foundation of China (NSFC) (62174166, 11991063, U2241219), Shanghai Municipal Science and Technology Major Project (2019SHZDZX01, 22JC1402902), and the Strategic Priority Research Program of Chinese Academy of Sciences (XDB43010200).

Biography: SUN Jing-Hua (1997-), male, Weifang, Shandong Province, Postgraduate, Research area involves single photon detection, E-mail: sjh_0702@163.com.

* **Corresponding author**: E-mail: wangwj@mail.sitp.ac.cn

Introduction

As a spatial exploration technology, remote sensing has gone through three stages: ground-based, airborne, and space-based. With increasing demands for detection distance and sensitivity in space remote sensing, infrared detectors with single-photon detection performance are urgently needed. Near-infrared InGaAs(P)/InP single-photon avalanche diodes(SPADs) have attracted wide attention in the field of space remote sensing due to small size, low power consumption, stable operation, and insensitivity to ultra-low operating temperatures[1-2]. However, in the complex space environment, many high-energy particles such as electrons, protons, neutrons, and heavy ions[3-5] create a radiation environment in which photodetectors experience displacement, total-ionization-dose, and single-event effects. These will temporarily or even permanently damage the performance of the detector, leading to performance degradation or even failure[6-9]. Therefore, in order to verify the reliability of the detector's operation in space, it is necessary to study how radiation affects device performance[10].

There have been various studies on the radiation resistance of InGaAs(P)/InP photodiodes. For example, Harris et al. investigated how proton and gamma irradiation affected the performance of an InGaAs avalanche photodiode (APD)[11-12]: under proton irradiation with an energy of 63 MeV and an incident flux of 2×10^{12} P/cm^2, the dark current of the detector increased from 5.6 nA to 1μA. Under gamma irradiation with a total dose of 269 krad (Si), the dark current of the detector increased from 0.1 nA to 1 nA. In addition, Zhang et al. gamma-irradiated an InGaAs p-i-n photodiode with a radiation dose rate of 16 rad (Si)/s and a total radiation dose of 30 krad (Si), and the results showed that the dark signal of the detector increased slightly after irradiation[13].

Previous studies on γ-irradiation of InGaAs(P)/InP photodetectors have mainly focused on p-i-n photodiodes or APDs, with little research on SPADs. In this paper, InGaAsP/InP SPADs were gamma-irradiated with 60 Co at different irradiation doses and dose rates, and the dark current, the photon detection efficiency (PDE), the after pulse probability (APP), and the dark count rate (DCR) were compared to analyze how gamma radiation affected the performance of InGaAsP/InP SPADs.

1 Irradiated samples and experiments

1.1 Device structure

The APD chip is composed of a separate absorption, grading, charge, and multiplication (SAGCM) heterostructure, as shown in Fig. 1(a). Epitaxial materials were sequentially grown on n-doped InP substrate: n^--doped InP buffer layer, intrinsic InGaAsP absorption layer, InGaAsP grading layer, n^+-doped InP charge layer, and intrinsic InP cap layer. In the undoped InP cap layer, the deep and shallow diffusion of Zinc formed a double p-type diffusion, which controlled the photosensitive surface diameter of the chip to 80 μm. Here, a charge layer is added to balance the electric field between the absorption and the multiplication layers. The electric field in the absorption region is kept small to suppress the generation of tunneling dark current. While the electric field in the multiplication region is kept large to ensure sufficient impact ionization for the photoexcited carriers, which generates a macroscopic current and achieves single photon detection capability. After surface passivation, a p-contact electrode was selectively grown on the p- region, and gold was deposited on the back-side of the substrate as the n-electrode, as shown in Fig. 1(b). The APD chip was packaged in a standard TO-66 metal tube shell, which integrated a three-stage thermoelectric cooler, as shown in Fig. 1(c).

1.2 Irradiation conditions

The irradiation source was a 60 Co point source with an intensity of 140 000 Ci, and all irradiations were performed at room temperature. According to the spatial application requirements of InGaAsP/InP SPADs, they should be able to work normally at an radiation dose rate of 5 krad (Si)/h and a total dose of 10 krad (Si). Therefore, the detectors were exposed at a dose rates of up to 50 krad (Si)/h and a total dose of up to 20 krad (Si).

Five devices with similar single-photon performance were selected from the same batch for irradiation experiments. The irradiation conditions were summarized in Table 1. Device1# and 2# were irradiated with a dose rate of 5 krad (Si)/h and a radiation dose of 10 krad (Si). Device 3# was irradiated with a dose rate of 50 krad (Si)/h and the radiation doses were 1/7/10/20/50/70 krad (Si). Device 4# was irradiated with a dose rate of 50 krad (Si)/h and a radiation dose of 10 krad (Si). Device 5# was irradiated with a dose rate of 50 krad (Si)/h and a radiation dose of 20 krad (Si). Among them, Device1# and 3# were biased at 0.95 V_{br} (breakdown voltage). Device 3# was tested in situ, while the others were performed with shift testing.

1.3 Test parameters

We tested the SPADs' dark currents in linear mode and the single-photon performances in Geiger-mode before and after irradiations, including PDEs, APPs, and DCRs. The dark current was tested using a Keithley 2635B programmable source meter. To test the single-photon performance, we built a pulse-gated single-photon test system as shown in Fig. 2. The signal generator (SG) generated two synchronizing signals: one was sent to the APD with a frequency of 1 MHz. The other was sent to the laser with a frequency of 200 kHz. The amplitude of the pulse voltage was 5 V with a pulse width of 4 ns. The light generated by the laser was calibrated to an average power of 0.1 photons per pulse after two-stage attenuation.

2 Experimental results and analysis

2.1 Influence of Gamma irradiation on dark current

Fig. 3 showed the dark current of Device 1# and 2# before and after irradiation. It can be seen that the dark current of the devices remained unchanged when the dose rate was 5 krad (Si)/h and the irradiation dose was

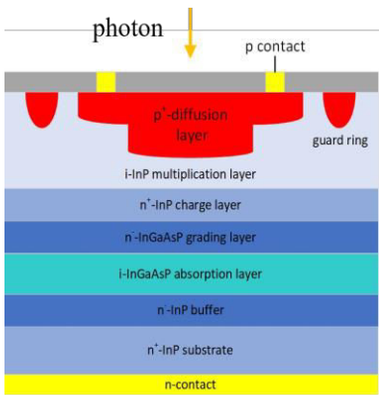

(a)

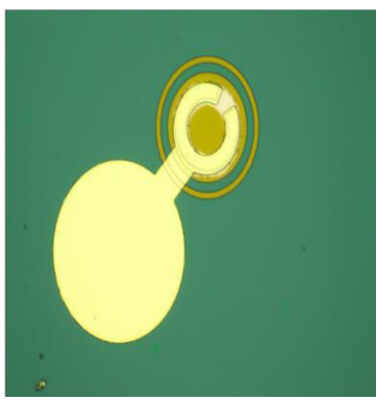

(b)

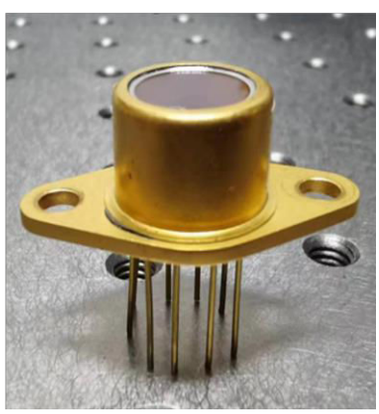

(c)

Fig. 1 Schematic of a TO-66 packaged InGaAsP/InP single-photon avalanche diode (SPAD): (a) Cross-sectional schematic of the InGaAsP/InP APD structure; (b)APD chip; (c) Physical appearance

图1 TO-66封装的InGaAsP/InP单光子雪崩探测器(SPAD)原理图: (a) InGaAsP/InP APD结构截面示意图; (b) APD 芯片; (c) 物理外观

10 krad (Si).

During irradiation, high-energy particles incident on the device lose energy due to ionization processes and generate electron-hole pairs in the material. If the rate of introducing electron-hole pairs is lower than the recombination rate, the performance of the device will tend to rapidly stabilize, which typically occurs within a few seconds to minutes after irradiation[14]. To illustrate this possibility, an in-situ experiment was conducted on Device 3#. The irradiation dose rate remained at 5 krad (Si)/h. When the irradiation dose reached 1/7/10/20/50/70 krad (Si), the device was taken out and tested as soon as possible within 15 minutes. Fig. 4 shows the dark current of Device 3# during the in-situ test. It can be seen that when the irradiation dose rate was fixed at 5 krad (Si)/h, the APD's dark current did not change with the increase of irradiation dose. Therefore, for a low irradiation dose rate, the electron-hole pairs introduced by irradiation will tend to recombine in a very short time without causing too much impact on the device performance.

Becker et al. subjected InGaAs APDs to gamma irradiation with doses ranging from 1 krad to 200 krad (Si): the maximum change in dark current after irradiation was 10 nA. However, Becker et al. did not specify the dose rate they used. We increased the dose rate from 5 to 50 krad (Si)/h and raised the total dose for Devices 4# and 5# to 10 krad (Si) and 20 krad (Si), respectively. The dark current of each device was tested before and after irradiation, and the results were shown in Fig. 5. As shown in Fig. 5(a), the dark current remained un-

Table 1 Summary of irradiation conditions
表1 样品辐照条件

Device	Radiation dose/ [krad (Si)]	Dose rate/ [krad (Si)/h]	Voltage/V
1#	10	5	0.95 V_{br}
2#	10	5	–
3#	1/7/10/20/50/70	5	0.95 V_{br}
4#	10	50	–
5#	20	50	–

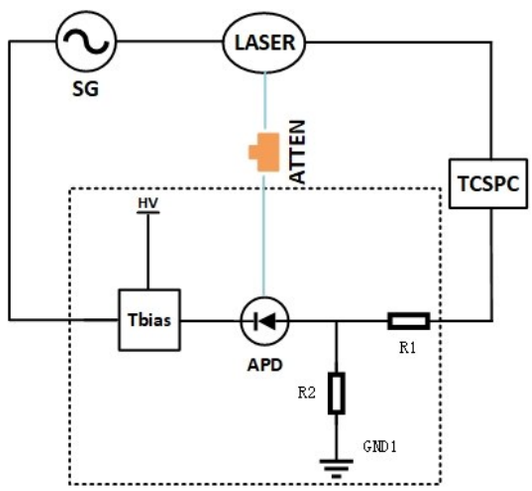

Fig. 2 Schematic diagram of gated-mode single-photon detection system

图2 门控模式单光子探测系统原理图

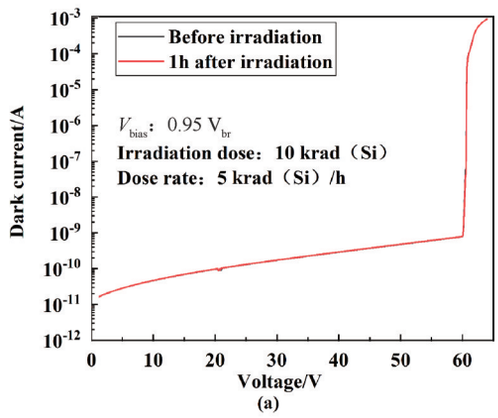

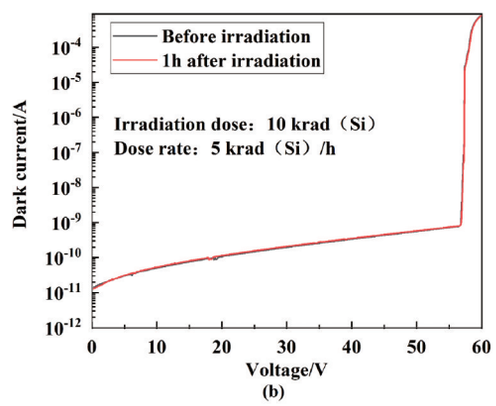

Fig. 3 Dark current before and after irradiation: (a) Device 1#; (b) Device 2#
图3 辐照前后暗电流: (a) Device 1#; (b) Device 2#

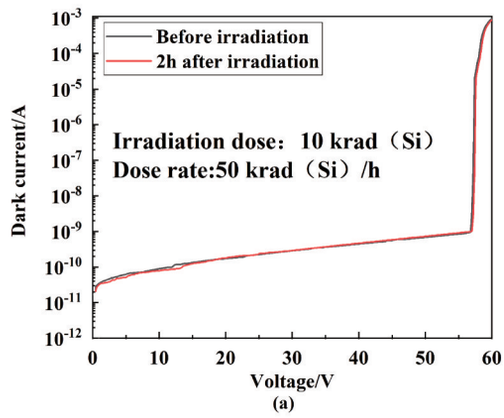

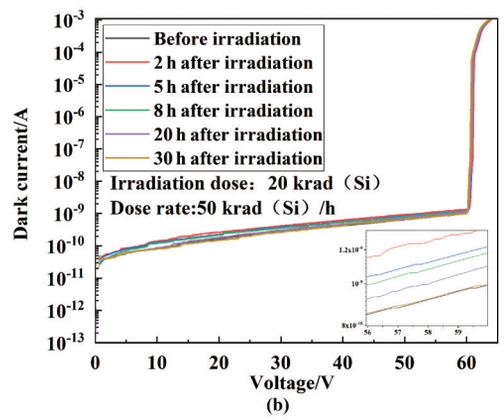

Fig. 5 Dark current before and after irradiation: (a) Device 4; (b) Device 5
图5 辐照前后暗电流: (a) Device 4#; (b) Device 5#

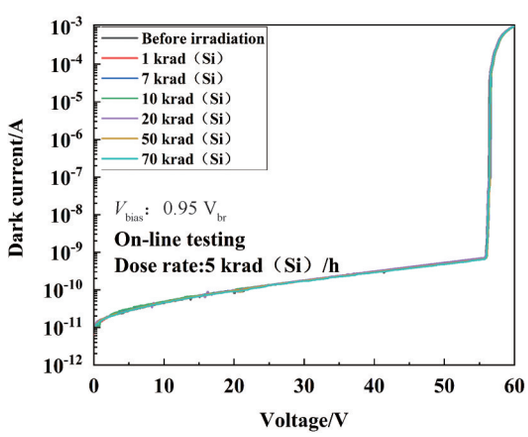

Fig. 4 Results of the dark current by in-situ test (Device 3#)
图4 Device 3# 原位测试暗电流曲线

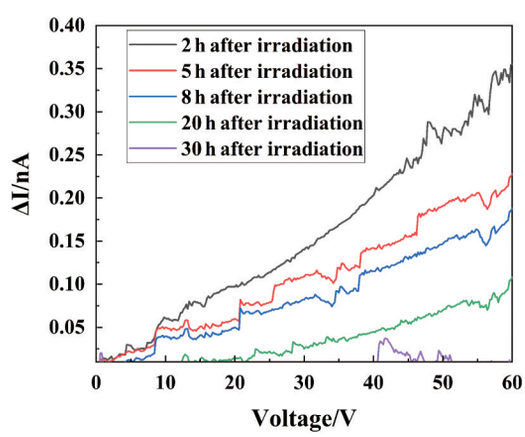

Fig. 6 Change of the dark current increment before and after irradiation for Device 5#
图6 Device 5#辐照前后暗电流增量变化

changed at a dose rate of 50 krad (Si)/h and an irradiation dose of 10 krad (Si). However, as shown in Fig. 5 (b), when the irradiation dose reached 20 krad (Si), the dark current of the Device 5# at 0.95 V_{br} increased by 1.4 times after irradiation. In the subsequent room temperature annealing process, the dark current gradually recovered and returned to the pre-irradiation level after 30 hours. Fig. 6 showed the change of the dark current increment (ΔI) of Device 5# before and after irradiation. It can be seen that ΔI increased with the increase of the bias voltage, which was throughout the entire voltage range. For an APD, as the bias voltage increases, the depletion layer gradually expands from the multiplication

layer to the absorption layer. The increment of the dark current caused by irradiation started from zero bias voltage, indicating that the ionization-induced electron-hole pairs were distributed throughout the device.

As the electric field increased, the depletion layer gradually increased, collecting more and more electron-hole pairs caused by irradiation. As shown in Fig. 6, after 2 hours of irradiation, ΔI increased by 0.094 nA in the range of 0-20 V, 0.106 nA in the range of 20-40 V, and 0.152 nA in the range of 40-60 V. The slow growth rate of ΔI represented a small multiplication.

Next, we will describe in detail the effects of irradiation on single-photon performance, such as PDE, DCR, and APP. It should be noted that these parameters after irradiation were obtained by shift testing 2 hours after irradiation.

2.2 Influence of Gamma irradiation on photon detection efficiency

For a SPAD, PDE is defined as the probability of detecting an incident single photon, which consists of three parts: quantum efficiency, i.e., the photoelectric conversion efficiency of incident photons. This is mainly related to parameters such as the probability of optical coupling, the thickness of the absorption layer, and the absorption efficiency of the material. Another part is the probability of photo-excited carriers injecting into the multiplication layer, and the other is the probability of carriers injected into the multiplication layer to trigger avalanche breakdown which is determined by the electric field and the thickness of the multiplication layer.

As can be seen in Fig. 7, the PDEs were basically unchanged after irradiation. The PDEs in Fig. 7(a) and Fig. 7(c) fluctuated slightly and irregularly, with the maximum change of only 1.64%, which were caused by the inconsistent testing environments before and after irradiation and the testing errors. Photon absorption is an inter-band process. The collection and multiplication processes are controlled by the electric field and will not be affected by the electron-hole pairs generated by irradiation[11]. Therefore, the PDEs will not change due to radiation, unless the radiation causes a strong recombination enhancement effect, which generally occurs in the displacement damage.

2.3 Influence of Gamma irradiation on after pulse probability

The APP is also an important parameter for an SPAD, which represents the false avalanche probability caused by the release of captured carriers due to defects in the SPAD material in the absence of photon incidence. Fig. 8 shows the APPs before and after irradiation. As can be seen, the APPs did not change significantly after irradiation, only fluctuated slightly without obvious regularity. Under a dose rate of 50 krad (Si)/h and an irradiation dose of 20 krad (Si), the dark current

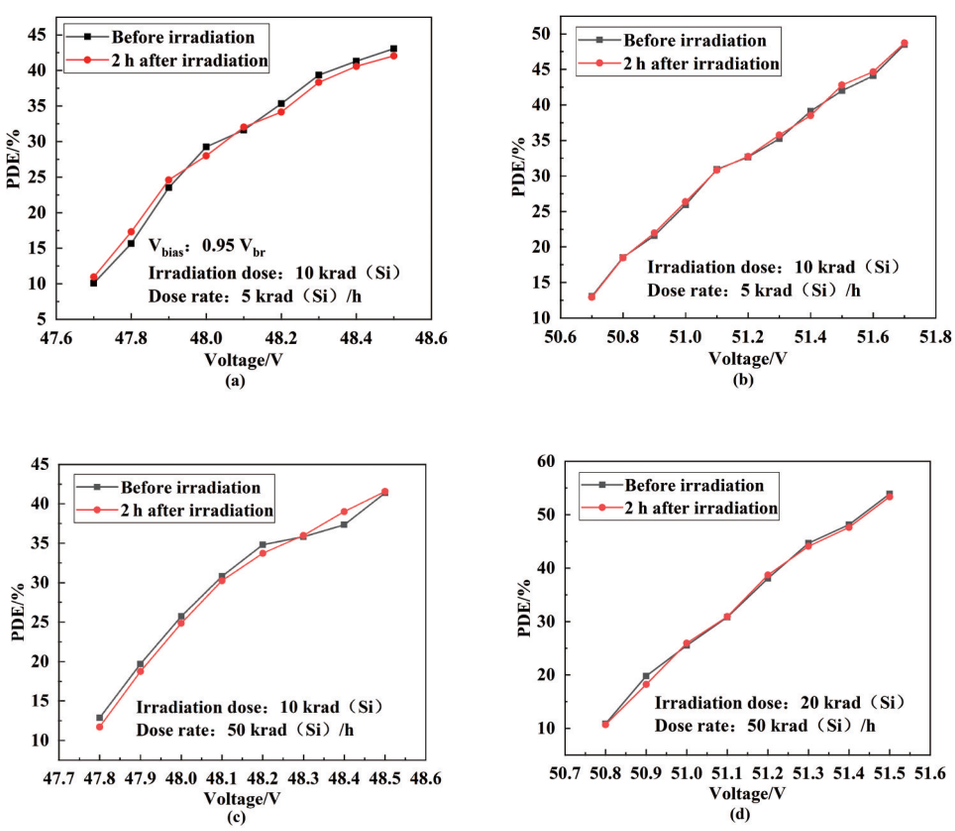

Fig. 7 PDEs of SPADs before and after irradiation: (a) Device 1#; (b) Device 2#; (c) Device 4#; (d) Device 5#

图7 辐照前后SPAD探测效率变化曲线: (a) Device 1#; (b) Device 2#; (c) Device 4#; (d) Device 5#

of the APD increased by 1.4 times after irradiation, as shown in Fig. 5(b), while the PDE and APP, as shown in Fig. 7(d) and Fig. 8(d), remained unchanged. The irradiation may cause ionizing damage and displacement damage to APDs. The ionization process is the interaction between high-energy particles and atomic electrons, producing electron-hole pairs. It is a transient change and will not cause permanent damage to the material properties. In contrast, displacement damage creates vacancies and interstitials, that is, permanent lattice defects[14]. The PDEs and APPs had no obvious changes, which meant that the device was free from irreversible damage such as defects to the material. Therefore, the main damage caused by gamma radiation to the SPADs was ionization damage, which corresponded to the dark current that recovered within a certain period of time.

3.4 Influence of Gamma irradiation on dark count rate

Fig. 9 shows DCRs of the SPADs before and after irradiation. In order to better compare the changes in DCR, the PDE of each device was fixed at 40%, and the detailed changes in DCR were listed in Table 2. It can be seen that 2 hours after irradiation with a dose of 10 krad (Si) and a dose rate of 5 krad (Si)/h, the DCRs of Device 1# and 2# increased by 1.36 and 1.30 times, respectively, and then began to recover to the level of non-irradiation until 48 hours after irradiation. Meanwhile, under the irradiation doses of 10 k/ 20 krad (Si) and a dose rate of 50 krad (Si)/h, the DCRs of Device 4# and 5# increased by 1.30 and 1.58 times, respectively, and then began to recover to the level of non-irradiation until 120 hours after irradiation. After irradiation, the dark current of Device 1#, 2#, and 4#, did not change, but the DCRs increased slightly. This was because the previously observed dark current was a parameter in the linear mode, where the multiplication factor was small, and the generation and recombination processes of electron-hole pairs can be offset. While in the Geiger-mode, due to a huge multiplication factor, the generated electron-hole pairs are greatly multiplied, which exceeds their recombination probability, and this is reflected in the DCR.

The difference in DCR and recovery time between Device 4#/5# and Device 1#/2# was mainly due to the difference in total radiation dose and the dose rate. As the radiation dose rate increased, the generation rate of electron-hole pairs exceeded the recombination rate, resulting in a multiplication process in the depletion layer and a longer time to recover to the non-irradiation level. In addition, as the total radiation dose increased, the number of generated electron-hole pairs increased, resulting in more obvious changes in DCR.

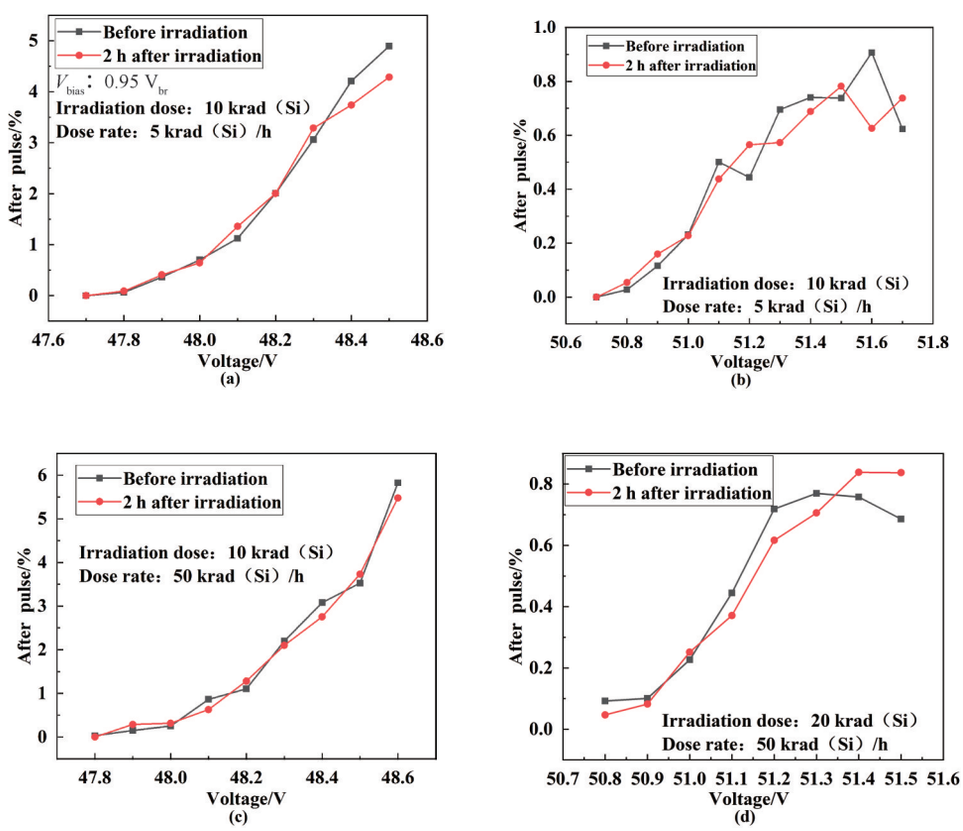

Fig. 8 PDEs of SPADs before and after irradiation: (a) Device 1#; (b) Device 2#; (c) Device 4#; (d) Device 5#
图 8 辐照前后 SPAD 后脉冲概率变化曲线: (a) Device 1#; (b) Device 2#; (c) Device 4#; (d) Device 5#

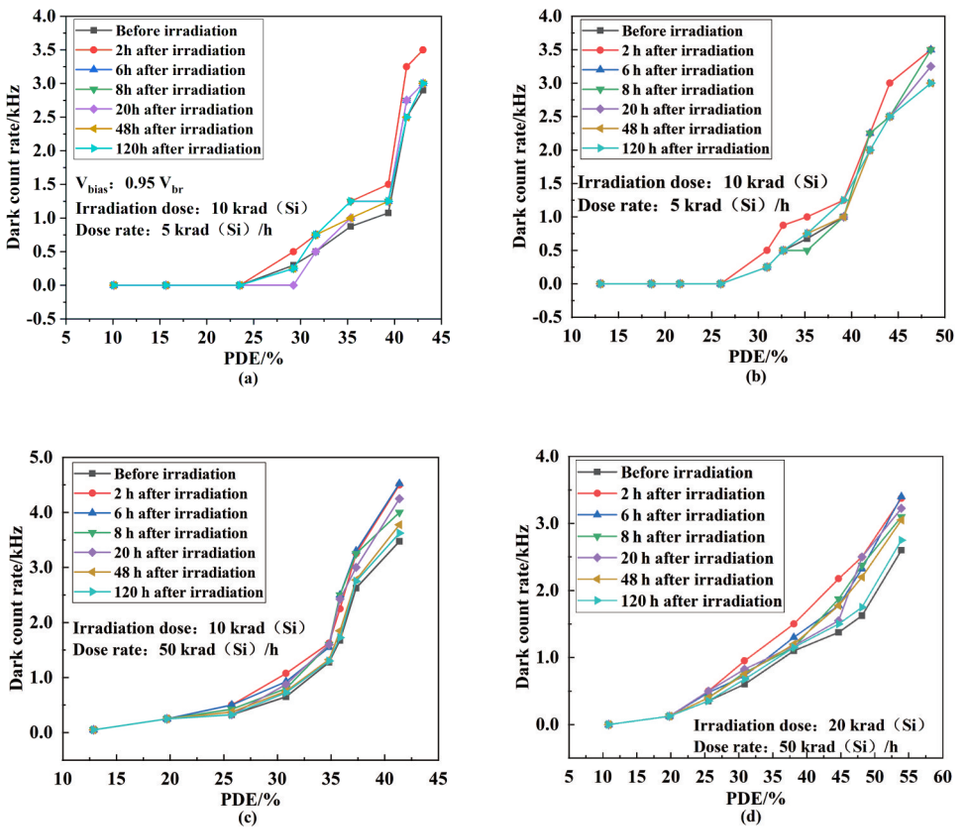

Fig. 9 DCRs of SPADs before and after irradiation: (a) Device 1#; (b) Device 2#; (c) Device 4#; (d) Device 5#
图9 辐照前后SPAD暗计数率变化曲线: (a) Device 1#; (b) Device 2#; (c) Device 4#; (d) Device 5#

Table 2 Change of DCR after irradiation at 40% PDE
表2 在PDE 40%时DCR的变化情况

Device	Radiation dose/ krad (Si)	Dose rate/ [krad (Si)/h]	DCR before irradiation/kHz	DCR 2 h after irradiation/kHz	Change factor	Recovery time/h
1#	10	5	1.1	1.5	1.36	48
2#	10	5	2.5	3.25	1.30	48
4#	10	50	3.47	4.5	1.30	120
5#	20	50	1.375	2.175	1.58	120

3 Conclusions

In this paper, InGaAsP/InP SPADs were gamma-irradiated at different doses and dose rates. At a radiation dose of 10 krad (Si), there were no changes in the dark current, PDE and APP, only a slight increase in DCR, which basically recovered to the non-irradiation level within a few days. When the radiation dose was increased to 20 krad (Si), the dark current and the DCR began to increase and gradually recovered after annealing at room temperature. The analysis indicated that the performance degradation of the device was mainly caused by ionization damage from gamma irradiation in the bulk material, resulting in many electron-hole pairs and a short-term degradation of device performance. During subsequent room temperature annealing, the device performance recovered to the level of non-irradiation due to the recombination of non-equilibrium carriers.

References

[1] Huang X, Li X, Shi M, *et al*. Effect of proton irradiation on extended wavelength In0.83Ga0.17As infrared detector [J]. *Infrared Physics & Technology*, 2015, **71**: 514-517.
[2] Kleipool Q L, Jongma R T, Gloudemans A M S, *et al*. In-flight proton-induced radiation damage to SCIAMACHY's extended-wavelength InGaAs near-infrared detectors [J]. *Infrared Physics & Technology*, 2007, **50**(1): 30-37.
[3] Chen H, Jiang M, Sun S, *et al*. Room temperature continuous frequency tuning InGaAs/InP single-photon detector [J]. *AIP Advances*, 2018, **8**(7).075106
[4] Zhou M, Wang W, Qu H, *et al*. InGaAsP/InP single photon avalanche diodes with ultra-high photon detection efficiency [J]. *Optical and Quantum Electronics*, 2020, **52**(6),299.
[5] Stassinopoulos E G, Raymond J P. The space radiation environment for electronics [J]. *Proceedings of the IEEE*, 1988, **76**(11): 1423-1442.
[6] Bourdarie S, Xapsos M. The near-earth space radiation environment

[J]. *IEEE Transactions on Nuclear Science*, 2008, **55**(4): 1810-1832.
[7] Benfante M, Reverchon J L, Gilard O, *et al*. Electric field enhanced generation current in proton irradiated InGaAs photodiodes[J]. *IEEE Transactions on Nuclear Science*, 2023.
[8] Nelson G T, Ouin G, Polly S J, *et al*. In Situ deep-level transient spectroscopy and dark current measurements of proton-irradiated InGaAs photodiodes[J]. *IEEE Transactions on Nuclear Science*, 2020, **67**(9): 2051-2061.
[9] Gilard O, How L S, Delbergue A, *et al*. Damage factor for radiation-induced dark current in InGaAs photodiodes[J]. *IEEE Transactions on Nuclear Science*, 2018, **65**(3): 884-895.
[10] Olantera L, Bottom F, Kraxner A, *et al*. Radiation effects on high-speed InGaAs photodiodes[J]. *IEEE Transactions on Nuclear Science*, 2019, **66**(7): 1663-1670.
[11] Harris R D, Farr W H, Becker H N. Degradation of InP-based Geiger-mode avalanche photodiodes due to proton irradiation [J]. *Journal of Modern Optics*, 2011, **58**(3-4): 225-232.
[12] Becker H N, Johnston A H. Dark current degradation of near infrared avalanche photodiodes from proton irradiation [J]. *IEEE Transactions on Nuclear Science*, 2004, **51**(6): 3572-3578.
[13] Zhang Hang, Liu Dongbin, Li Shuai, *et al*. Analysis of total dose irradiation test for InGaAs detector[J]. *Journal of Transduction Technology*,(张航, 刘栋斌,李帅,等. InGaAs探测器总剂量辐照性能试验分析 [J]. **传感技术学报**),2015, **28**(1): 19-22.
[14] Srour J R, Marshall C J, Marshall P W. Review of displacement damage effects in silicon devices [J]. *IEEE Transactions on Nuclear Science*, 2003, **50**(3): 653-670.